Novel Nickel Foam with Multiple Microchannels as Combustion Reaction Support for Self-heating Methanol Steam Reforming Microreactor

Tianqing Zheng[a], Wei Zhou[a] *, Yifan Yang[a], Yuchen Zhong[a], Huihui You[a], Xinying Li[a], Xuyang Chu[a], Kwan San Hui[b], Weihua Ding[c]

[a] *Department of Mechanical & Electrical Engineering, Xiamen University, Xiamen 361005, China*

[b] *School of Mathematics, University of East Anglia, Norwich, NR4 7TJ, United Kingdom*

[c] *Rison Hi-tech Materials Company Limited, Yiwu 322000, China*

Abstract: To improve hydrogen production performance of self-heating methanol steam reforming (MSR) microreactor, a novel nickel foam with multiple microchannels was proposed as combustion reaction support. A wall temperature comparison of the methanol combustion microreactors with nickel foam catalyst support and particles catalyst support in the combustion reaction process was performed. According to the numerical simulation results of combustion reaction of nickel foam, the shape and size of multiple microchannels of nickel foam were determined. The laser processing was then used to fabricate the multiple microchannels of nickel foam. The experimental results show that the methanol combustion microreactor with nickel foam loaded with Pt catalyst exhibits similar wall temperature distribution with the methanol combustion microreactor with Pt/γ-Al_2O_3 particles reaction support. Compared with the nickel foam without microchannel, the ΔT_{max} (maximum temperature difference) and the maximum in the temperature distribution of nickel foam with multiple microchannels decreased respectively by 57.8% and 33.8 ℃ when 1.1 mL/min methanol flow rate was used. Hydrogen production performance of self-heating MSR microreactor using the nickel foam with multiple microchannels increased by about 21% when 430 ℃ reforming temperature and 4 mL/h methanol-water mixture flow rate were performed.

Keywords: Methanol steam reforming; Methanol combustion; Nickel foam; Multiple microchannels

---

*Corresponding author. Tel.: 86-592-2188698; Fax: 86-592-2186383

E-mail address: weizhou@xmu.edu.cn (Wei Zhou).

Nomenclature

Variables

K Kelvin environmental temperature of methanol steam reforming, K

m volume fraction of CO in reaction product, %

n volume fraction of CO_2 in reaction product, %

V_{H2} flow rate of H_2, mol/h

$V_{injection}$ flow rate of the methanol-water mixture, mL/h

$V_{reactant}$ flow rate of reactant, mL/min

X_{CH3OH} methanol conversion, %

z volume fraction of H_2 in reaction product, %

Abbreviations

EDS energy dispersive spectrometer

MC methanol combustion

MSR methanol steam reforming

PPI pores per inch

SEM scanning electron microscopy

ΔT_{max} maximum temperature difference

1. Introduction

Methanol steam reforming (MSR) microreactor is used as one of the main technology for hydrogen production because of its high ratio of hydrogen to carbon[1-5], easy storage and transportation[6], low reforming temperature[6]. The MSR microreactor using fuel as its heat-supply mode has a wide application in fuel cell[7-11] owing to little electrical power consumption, it has been paid much attentions from scholars.

The MSR microreactor using fuel as its heat-supply mode has been widely studied, including some researches such as heat-supply mode, catalyst for combustion, catalyst support for combustion. In the heat-supply mode, the fuels of butane, propane and methanol have been studied to realize the heat-supply of MSR microreactor[12-15]. As for the combustion catalyst, the effects of catalyst composition, catalyst preparation process, and catalyst reaction condition on the catalytic performance of catalyst have been investigated. The catalysts with different activities have been obtained, such as Pd/ZrO_2, Pt/Al_2O_3 and Mn/Cu catalysts[16-18].

In terms of catalyst support for combustion, the spherical particles and metal plate with microchannels were investigated[13,19]. For example, Chein *et al.* used Pt/Al_2O_3 particles as combustion reaction support for the heat-supply of MSR reaction. The 97% conversion of the reforming methanol can be obtained[13]. Reuse *et al.* used FeCrAlloy metal plate with microchannels as catalyst support, which was loaded with highly active cobalt oxide catalyst, for the heat-supply of MSR reaction. It was found that more than 99% reforming methanol conversion can be obtained at the reforming temperature higher than 250 °C[19]. The wall temperature and combustion methanol conversion of the self-heating MSR microreactor with combustion catalyst support were investigated in the above studies. However, the temperature distribution of the combustion catalyst support has not been studied in detail. A few research works on temperature distribution optimization of hydrogen production microreactor have been done by some research groups[20-21]. For example, Hsueh et al. used numerical simulations to investigate mass-transfer and heat-transfer performances of self-heating MSR microreactor. It was found that the countercurrent configuration of MSR gas and methanol combustion (MC) gas can increase reaction performance of the microreactor[20]. Herdem et al. used numerical simulation to investigate temperature distribution of MSR microreactor. It was found that temperature distribution of MSR microreactor was an important influential factor in improving the reaction performance of the reactor[21].

Although some research works on heat-supply method, catalyst and catalyst support for combustion have been performed, the temperature distribution optimization of the self-heating MSR microreactor using metal foam as combustion reaction support has not been studied in detail. In fact, compared with the traditional packed bed system, the metal foam used as reaction support in the microreactor has the advantages of lower pressure drop and less cold spots[22]. Moreover, the catalyst support of metal foam was easy to be secondary processed by laser, thus it can easily achieve the fabrication of the optimized structure of reaction support, so as to perform the difference decrease in the temperature distribution of the catalyst support. In addition, the metal foam has strong catalytic reaction ability because of its large specific surface area. Therefore, the nickel foam was chosen as a research object of the MC catalyst support. The wall temperature distribution of methanol combustion microreactor with the nickel foam loaded with Pt catalyst was studied. A numerical simulation model of combustion reaction of the nickel foam was established. A structural optimization of the nickel foam reaction support was carried out to decrease difference in the temperature distribution of the nickel foam based on the numerical simulation model. The wall temperature distributions of methanol combustion microreactors with the nickel foams before and after structural optimization were investigated in detail. In addition, the reforming methanol conversion and H_2 flow rate of self-heating MSR microreactors with the nickel foams were studied.

2. Experimental and numerical setup

2.1. Nickel foam as combustion reaction support

It is difficult to locate the Pt/γ-Al_2O_3 particles in a chamber plate and change the distribution of these particles to optimize the temperature distribution, however the temperature distribution optimization of chamber plate needs change the particles distribution of Pt/γ-Al_2O_3 particles. Thus a metal foam was proposed to be used as catalyst support for combustion because of its advantages of rapid assembling ability, easy secondary processing ability which can achieve the temperature distribution optimization of chamber plate. In addition, the metal foam has the advantages of low pressure drop and large specific surface area. The copper foam becomes brittle at high temperature because its easy oxidation at high temperature and therefore is not suitable for being used as catalyst support for combustion. Ni-based foam and Fe-based foam have been used as combustion reaction supports by some scholars because of their good oxidation resistance and corrosion resistance[23-27]. For example, Cimino et al. investigated the methanol combustion reaction of Fecralloy foam loaded with Pt catalyst by cathodic electrodeposition[23]. The results showed that the initial temperature of methanol combustion reaction can be lower than 80 ℃, and the conversion of the methanol can reach 100% when the Pt content is 13 mg/cm^{-3}. Jin et al. studied the H_2 combustion reaction of nickel foam loaded with Pt catalyst[24]. It was found that the H_2 conversion of the nickel foam reaction support was higher than 99%. Yang et al. investigated the methane combustion reactions of the copper foam and the nickel foam loaded with Pt catalyst[25]. The result showed that the nickel foam had better catalyst adhesion and more heat release amount than copper foam in the combustion reaction. In this way, 110 PPI nickel foam with 0.2mm average pore size, 0.06mm average strut size and 98% porosity (purchased from Jia Yi Sheng Company, Jiangsu, China) is used as a research object of combustion reaction support.

2.2. Pressure drop test

Fig.1 shows the testing system of pressure drop of reaction support. This testing system mainly consists of inlet chamber plate, testing chamber plate, reaction support, outlet chamber plate, digital pressure gauge with 0.4% measurement precision (YB-100A, Suzhou Xuansheng Technology Company, China). The pressure drop of reaction support was investigated by comparing the pressure in the front of reaction support with the pressure in the back under different flow rates of air.

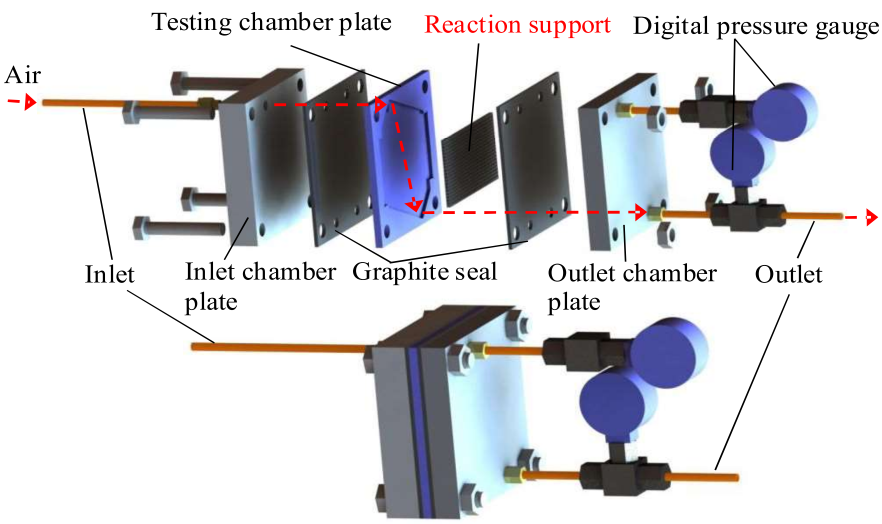

Fig.1. Testing system of pressure drop of reaction support

2.3. Catalyst loading process and adhesion test

5g commercial Pt/γ-Al_2O_3 (1 wt% Pt) catalyst particles with 2 mm diameter (purchased from Kaida Chemical Engineering Company, Shanxi, China) were ground for one hour in planetary ball mill instrument to obtain the Pt catalyst powder. The ground Pt catalyst powder was mixed with $Al(NO_3)_3·9H_2O$, CH_3OH, H_2O at a mass ratio of Pt catalyst powder : $Al(NO_3)_3·9H_2O$: CH_3OH : H_2O = 2 : 1 : 5 : 5 to prepare catalyst precursor slurry. In order to uniformly disperse the Pt catalyst powder in the precursor slurry, the precursor slurry was continuously stirred in a magnetic stirrer at room temperature.

The Pt catalyst was loaded on nickel foam by impregnation-dry method. The nickel foam was sufficiently impregnated in the catalyst precursor slurry and was then dried at 100℃ for 15 mins in an oven. The above operations were repeated until the slurry was consumed. The component of Pt catalyst on the nickel foam was analyzed by scanning electron microscopy (SEM). The adhesion of Pt catalyst on the nickel foam was investigated using ultrasonic cleaning machine at ultrasonic frequency of 40 kHz[9].

2.4. Numerical simulation model of combustion reaction

2.4.1. Physical model

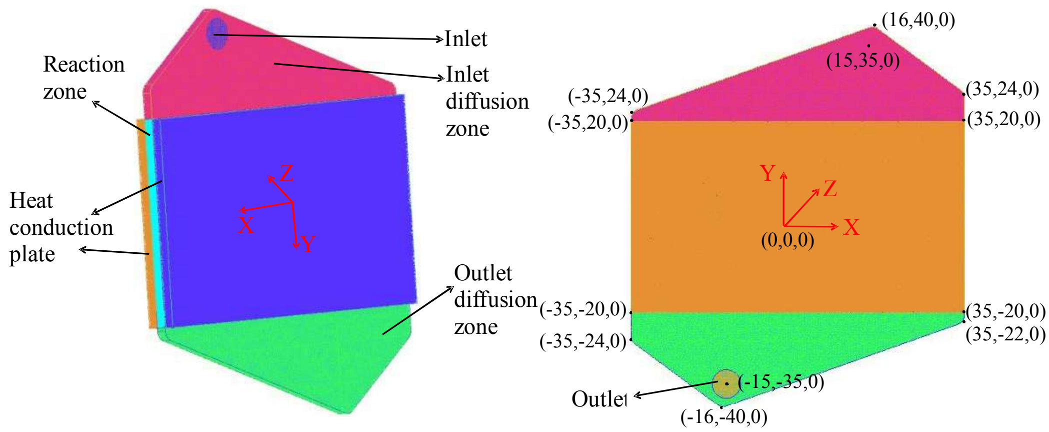

Fig.2. Computational domain composition of the numerical simulation model of combustion reaction

According to the composition of MC microreactor, the computational domain of simulation model for combustion reaction was divided into six parts: inlet, inlet diffusion zone, reaction zone, heat conduction plate, outlet diffusion zone and outlet, as shown in Fig.2. The flow velocity of methanol-air mixture which flowed through the reaction support was more than 0.1 m/s, therefore the Reynolds number of the fluid was more than 4000. In this way, the methanol-air mixture was regarded as the turbulent gas in numerical simulation of combustion reaction. The fluid flow in the nickel foam reaction support was simulated by a Darcy 's law (Eq.(1)). The flow behavior of the fluid can be described by Navier-Stokes equation (Eq.(2)) and Continuity equation (Eq.(3))[28]. The pre-exponential factor of methanol oxidation was set to 4e+06. The activation energy of methanol oxidation was set to 3.5e+07 J·kmol^{-1}.

$$v = -\frac{K \cdot \nabla P}{\mu} \tag{1}$$

$$(\nabla \cdot u) = -\nabla P + \mu \cdot \nabla^2 u \tag{2}$$

$$\nabla(\rho \cdot u) = 0 \tag{3}$$

2.4.2. Boundary condition

The boundary conditions of inlet and outlet were set to constant velocity and pressure-outlet, respectively. No slip was set as the boundary conditions of all walls and interfaces in the computational domain. The thermal conditions of all wall surfaces were set to mixed conditions with the 15 W·(m^2·k)$^{-1}$ heat-transfer coefficient, 300 k free stream temperature, 1 external emissivity and 573 k external radiation temperature. The reaction zone was set to the porous reaction zone with 98% porosity. The viscosity resistances of porous zone in X, Y and Z directions were set to 2.158e+09 m^{-2}. The inertial resistances of porous zone in X, Y and Z directions were set to 40928 m^{-1}.

2.4.3. Numerical solution condition

FLUENT 17.0 was used as numerical solution software. The QUICK scheme with SIMPLE algorithm was used for pressure-velocity coupling. The convergence criteria of pressure-based solver were set to 1e−05, and the under-relaxation factors of pressure, density and momentum were set to 0.35, 1, 0.5, respectively.

2.4.4. Grid independence analysis

ICEM CFD 17.0 was used to establish unstructured grids for discretization of the computational domain. The grid independence was investigated by comparing the simulation results of the simulation models with the grids of 630409, 877589, 1511424 and 2466095, respectively. According to the simulation calculation results, the average temperatures of the simulation models with grid numbers of 630409, 877589, 1511424 and 2466095 were 407.9 ℃, 393.1 ℃, 391.2 ℃ and 389.9 ℃, respectively. The average temperature difference between the grid numbers of 877589, 1511424 and 2466095 was less than 3%. Considering the calculation time and accuracy, the grid number of 1511424 was used. Moreover, according to the grid quality evaluation of ICEM CFD, the grid quality of the model with the grid number of 1511424 was greater than 0.3, so it met calculation accuracy requirement.

2.4.5. Reliability validation of numerical simulation model

The reliability of the numerical simulation model was verified by investigating the difference between simulation temperature and experimental temperature of nine points on combustion chamber plate of MC microreactor under methanol flow rates of 0.8, 0.9, 1.0 and 1.1 mL/min, respectively.

2.5 Structural optimization of nickle foam

In the reaction process of methanol combustion, the reaction occurs when reaction gas comes into contact with catalyst. A large amount of reaction gas is reacted with catalyst in the front of nickel foam loaded with catalyst because of the nickel foam's porous structure with small pore size and dense hole distribution. Therefore, the violent methanol combustion reaction in the front of the nickel foam is obtained. In this way, the temperature on the front of chamber plate with the nickel foam combustion reaction support was high, however that on the back was low. In order to optimize the temperature distribution of the chamber plate, it is necessary to control reaction zone of the reaction support. In fact, the distribution of reaction gas and catalyst in the reaction support can be adjusted by designing multiple microchannels on the reaction support. Therefore, the shape and size of multiple microchannels of the nickel foam were designed based on numerical simulation results of combustion reaction of nickel foam.

2.6. Combustion performance test

Fig.3 shows a methanol combustion microreactor and Fig.4 shows a testing system of methanol combustion microreactor[24]. The methanol for combustion was evaporated in the inlet evaporation chamber plate and combustion evaporation chamber plate, then was mixed with the air in the mixing chamber plate. Subsequently, the mixed gas was reacted with the combustion reaction support in the outlet chamber plate. The combustion reaction support in the microreactor had 70mm length, 40mm width, and 2mm thickness. The temperature inspection instrument with 0.1 ℃ measurement accuracy (AT4516, Applent Instruments Company, China) was used to investigate the temperatures of the different points on combustion chamber plate of the microreactor. The maximum difference and the maximum in the temperature distribution of the nine points were used for determining combustion performance of the microreactor[28]. The low maximum difference and the low maximum in the temperature distribution indicated the better combustion performance. Eq. (4) shows the MC reaction process[13,22].

$$CH_3OH + 1.5O_2 \rightarrow CO_2 + 2H_2O \quad \Delta H = -192.2\ KJ/mol \tag{4}$$

In this study, particles reaction support was the 5g Pt/γ-Al_2O_3 catalyst particles with 2 mm diameter. The same 5g Pt/γ-Al_2O_3 catalyst particles were ground to prepare catalyst precursor slurry and the Pt catalyst precursor slurry was then loaded on the nickel foam to obtain the nickel foam reaction support. The wall temperature of methanol combustion microreactor with nickel foam reaction support was compared with that of methanol combustion microreactor with particles reaction support under 0.8 mL/min flow rate of methanol, namely 3.93 L/min flow rate of methanol-air mixture gas (the mole ratio of gaseous methanol to air was 1:7.14). The wall temperature of methanol combustion microreactor with the nickel foam in the combustion reaction process under different flow rates of methanol was investigated. The long-time combustion stability of the nickel foam in condition of 1 mL/min flow rate of methanol was studied. In addition, a combustion performance comparison of nickel foams without microchannel and with multiple microchannels at different flow rates of methanol was performed .

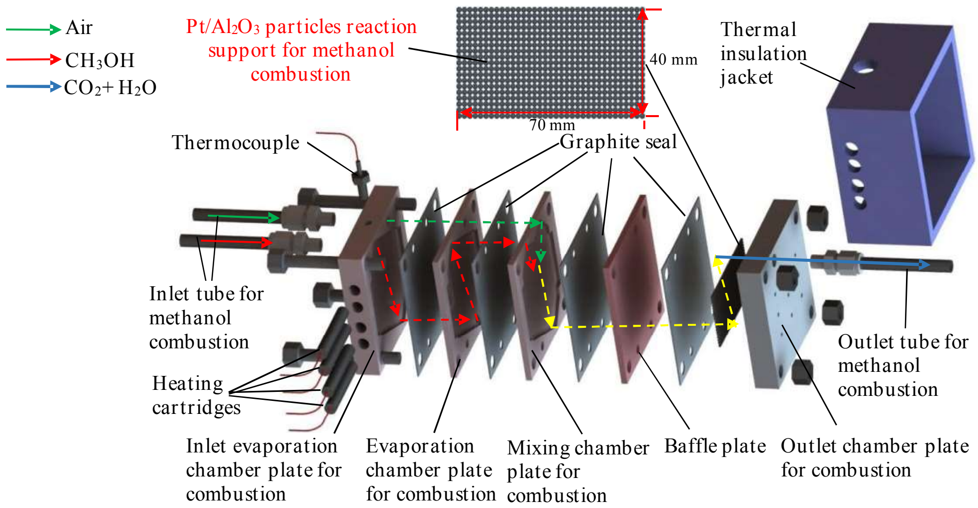

Fig.3. Methanol combustion microreactor

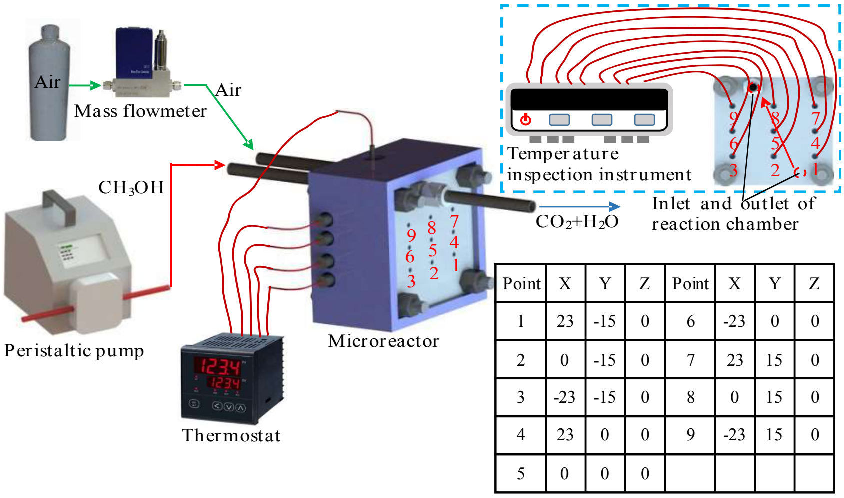

Point	X	Y	Z	Point	X	Y	Z
1	23	-15	0	6	-23	0	0
2	0	-15	0	7	23	15	0
3	-23	-15	0	8	0	15	0
4	23	0	0	9	-23	15	0
5	0	0	0				

Fig.4. Testing system of methanol combustion microreactor

2.7. Hydrogen production performance test

Fig.5 shows a self-heating methanol steam reforming microreactor and Fig.6 shows a testing system of self-heating methanol steam reforming microreactor[29]. The combustion methanol was evaporated in the inlet evaporation chamber plate and combustion evaporation chamber plate, then was mixed with air in the mixing chamber plate. The combustion reaction of methanol-air mixture occurred in the combustion reaction chamber plate. The methanol-water mixture was evaporated in the reforming evaporation chamber plate, then performed methanol steam reforming reaction in the reforming reaction chamber plate. The methanol combustion and methanol steam reforming reaction supports in the microreactor had 70mm length, 40mm width, and 2mm thickness. Pt/γ-Al_2O_3 catalyst particles in combustion chamber plate of the microreactor were used to supply heat to the reforming chamber plate[30-33]. The reforming temperature of the microreactor was measured using B-type thermocouple with 0.5 °C measurement accuracy (M6-K, Jing Lan Electric Heating Instrument Company, China) which was on the chamber plate for reforming. The MSR reactant was reacted with the PdZn catalyst which was on the copper foam in reforming chamber plate of the microreactor[34]. The soap bubble flowmeter with ±1% measurement deviation (JCL-2010(S)-A, Qingdao Juchuang Environmental Company, China) was used to investigate the flow rate of total reaction product, the gas chromatograph with 50 ppm measurement accuracy (GC2014C, Shimadzu Company, Japan) was used to determine the volume fractions of different reaction products [28].

Eqs.(5)-(7) show the main reaction process of MSR reaction[35-37]. The methanol conversion and H_2 flow rate were used as the main indices for determining hydrogen production performance of the microreactor, which were calculated using Eqs.(8) and (9)[7,9,29,38].

$$CH_3OH + H_2O \rightarrow 3H_2 + CO_2 \quad \Delta H = +49.4\ KJ/mol \tag{5}$$

$$CH_3OH \rightarrow CO + 2H_2 \quad \Delta H = +92.0\ KJ/mol \tag{6}$$

$$CO + H_2O \rightarrow CO_2 + H_2 \quad \Delta H = -41.1\ KJ/mol \tag{7}$$

$$X_{CH_3OH} = \frac{V_{reactant} * (m+n) * K}{V_{injection} * 1592.5} \tag{8}$$

$$V_{H_2} = \frac{V_{reactant} * z}{1344000} \tag{9}$$

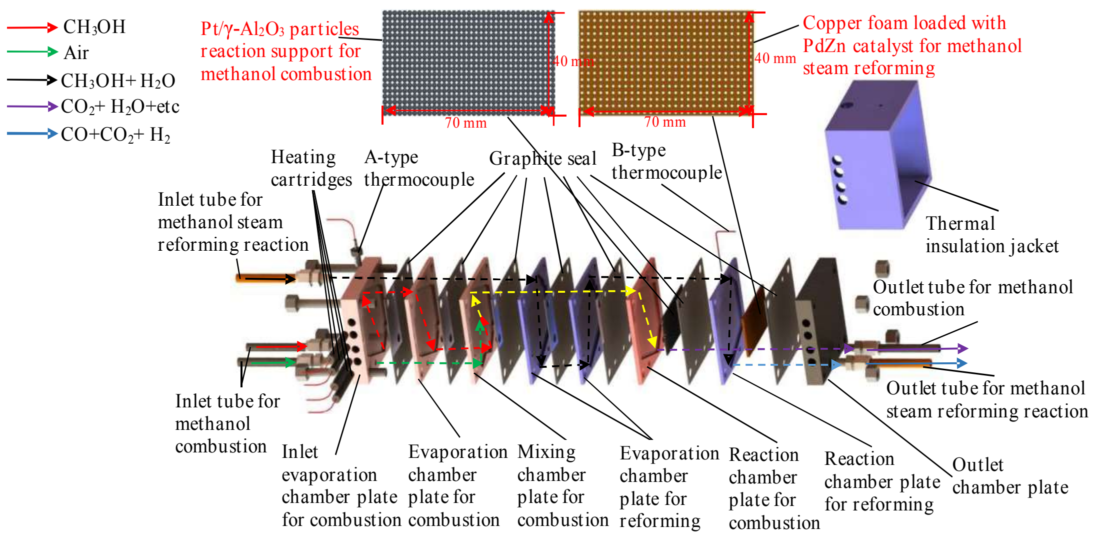

Fig.5. Self-heating methanol steam reforming microreactor

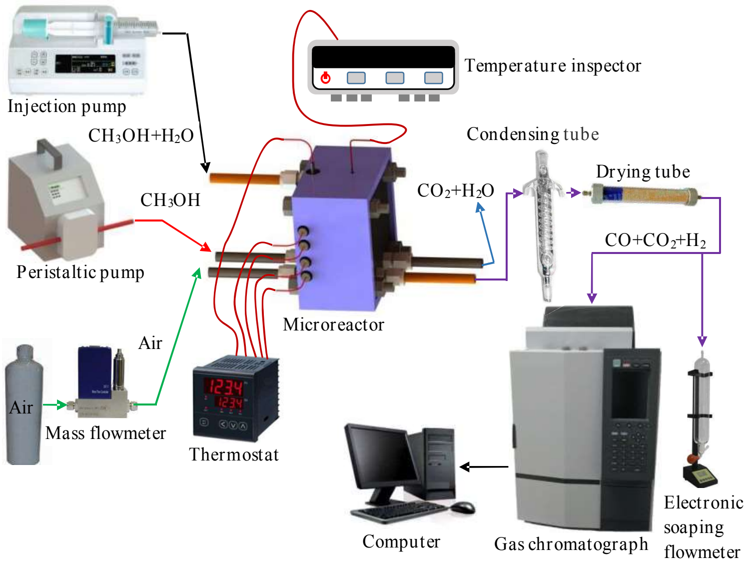

Fig.6. Testing system of self-heating methanol steam reforming microreactor

110 PPI copper foam which loaded 0.5 g PdZn catalyst was used as methanol steam reforming reaction support of self-heating MSR microreactor[34]. The nickel foams without microchannel and with multiple microchannels used as combustion reaction supports were respectively installed into the self-heating microreactors. The hydrogen production performances of the microreactors with different combustion reaction supports at different reforming temperatures and 4 mL/h flow rate of methanol-water mixture were investigated. Moreover, the hydrogen production performances of the microreactors under different flow rates of methanol-water mixture and 415 °C reforming temperature were also studied.

3. Results and discussion

3.1 Pressure drop of nickel foam

Fig.7 shows the pressure drop of different reaction supports under different flow rates of air. From Fig.7, it is found that the pressure drop of reaction supports becomes high with the increase of flow rate of air. Moreover, compared with particles reaction support, the nickel foam reaction support has the lower pressure drop.

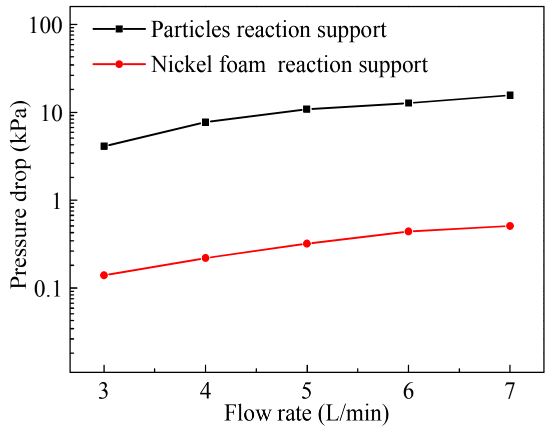

Fig.7. Pressure drop of different reaction supports under different flow rates of air

3.2. Catalyst adhesion of nickel foam

Fig.8 shows the catalyst adhesion of nickel foam. The Pt catalyst is loaded on nickel foam, as shown in Fig.8(a). According to Fig.8(b), it is known that some loss of catalyst occurs at the early stage of ultrasonic vibration process under five replicated experiments. The mass of catalyst remains basically unchanged at the later stage. In this way, the good catalyst adhesion of nickel foam can be concluded. This is mainly due to the presence of $Al(NO_3)_3$ binder in the catalyst precursor slurry, and the large specific surface area of the nickel foam, resulting in a large interfacial area of adhesion. Therefore, the catalyst had a high bonding strength with nickel foam. The good catalyst adhesion of nickel foam can be obtained.

(a)

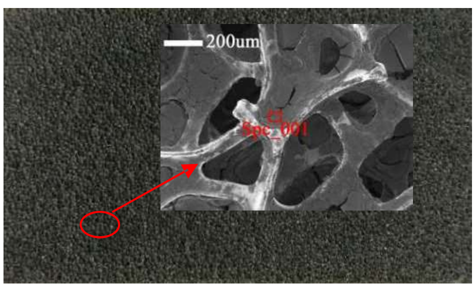

Name	C	O	Al	Ni	Pt	Total
Spc_001	1.96	58.70	36.03	2.51	0.80	100

(b)

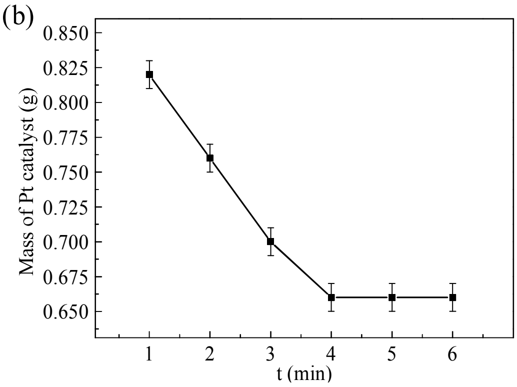

Fig.8. Catalyst adhesion of nickel foam: (a) SEM and energy dispersive spectrometer (EDS), (b) adhesion

3.3. Wall temperature of the methanol combustion microreactors with nickel foam

Fig.9 shows the wall temperatures of the methanol combustion microreactors with different catalyst supports. Compared with catalyst support of particles with 2 mm diameter, the higher temperature distribution is existed in the front (1-4 temperature measurement points) of the nickel foam catalyst support and the similar temperature distribution is existed in the back, which can be seen in Fig.9. It may be attribute to the fact that 110 PPI nickel foam has larger specific surface area because of its porous structure with small pore size and dense hole distribution[39-40]. Therefore, the violent combustion reaction was existed in the nickel foam loaded with Pt catalyst, especially in the front of the nickel foam.

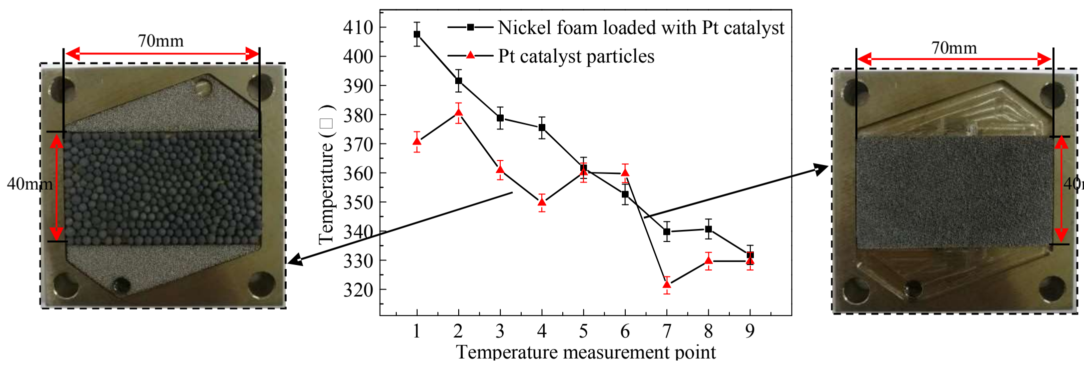

Fig.9. Wall temperatures of the methanol combustion microreactors with different catalyst supports

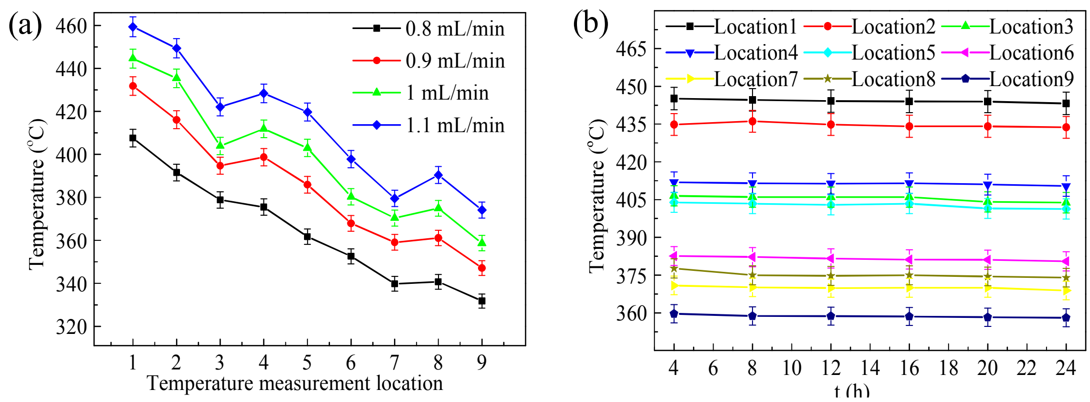

Fig.10. Wall temperature of the methanol combustion microreactor with nickel foam: (a) wall temperature under different flow rates of methanol (b) long-term wall temperature

Fig.10 shows the wall temperature of the methanol combustion microreactor with nickel foam. From Fig.10(a), it can be seen that with the increase of methanol flow rate, the temperatures of different measurement points increase, suggesting that the exothermic amount of the MC microreactor can be controlled by adjusting the flow rate of methanol. The temperatures of the nine points on combustion reaction chamber with the nickel foam remain basically unchanged within 24 hours combustion reaction, as shown in Fig.10(b), indicating that the nickel foam has good long-time combustion stability.

3.4. Reliability of numerical simulation model

Fig.11 shows the simulation and experimental temperatures of nine points on combustion chamber plate. The changing trend of the simulation temperatures of the nine points on combustion chamber plate under different flow rates of methanol is in agreement with the experimental temperatures, as shown in Fig.11. The deviations between simulation and experimental results of the minimum, maximum and average temperatures are 0.08%, 7.84%, 3.56%, respectively. Thus, the certain reliability of numerical simulation model is obtained.

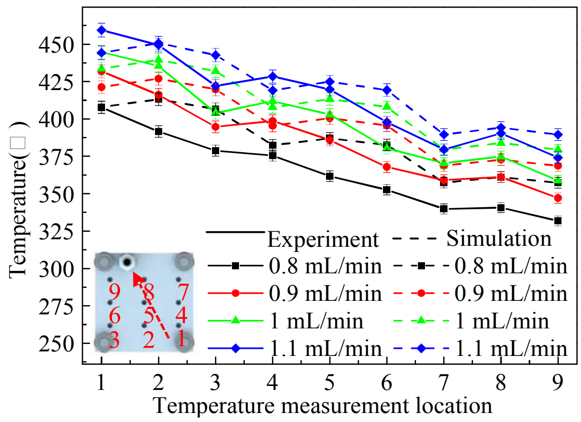

Fig.11. Simulation and experimental temperatures of nine points on combustion chamber plate

3.5. Numerical simulation of combustion reaction of nickel foam

Fig.12 shows the numerical simulation results of combustion reaction of nickel foam. From Fig.12, it can be seen that the high methanol concentration and temperature are existed in the front of nickel foam, however the low methanol concentration and temperature are existed in the back. A large amount of reactant reacts with catalyst in the front of nickel foam because of the nickel foam's porous structure with small pore size and dense hole distribution. The violent MC reaction in the front of the nickel foam is obtained. However, the less MC reaction occurs in the back of the nickel foam. In this way, the high temperature difference was emerged on the nickel foam. In order to decrease the difference in the temperature distribution of the chamber plate, it is necessary to control reaction zone of the reaction support. In fact, the distributions of reactant and catalyst in the reaction support can be adjusted by designing different multiple microchannels on the reaction support. Therefore, the multiple microchannels with specific shape and size were designed to investigate the effect of multiple microchannels on the temperature distribution of the nickel foam.

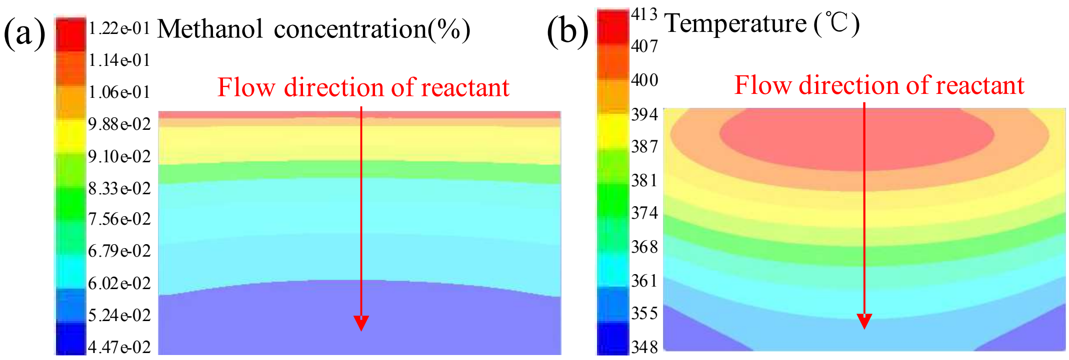

Fig.12. Numerical simulation results of combustion reaction of nickel foam: (a) methanol concentration, (b) temperature

3.6. Structural parameters of nickel foam with multiple microchannels

In order to reduce the difference in the temperature distribution of nickel foam, the amount of reactants which performs MC reaction in the front of the reaction support should be reduced, and the amount of reactants which performs MC reaction in the back of the reaction support should be enhanced. Therefore, the multiple microchannels with wide microchannel in the front of the nickel foam and narrow microchannel in the back of the nickel foam were designed on the nickel foam. Fig.13 shows the structural shape of multiple microchannels of nickel foam. The structural parameter A is the microchannel width which near the outlet of reaction chamber, the structural parameter B is the height of the microchannel, the structural parameter C is the distance between the edge of nickel foam and the centerline of the microchannel and the structural parameter α is the angle between the width direction and the longest side direction of the microchannel. A set of specific structural parameters of multiple microchannels of the nickel foam was determined, which is shown in the Tab.1.

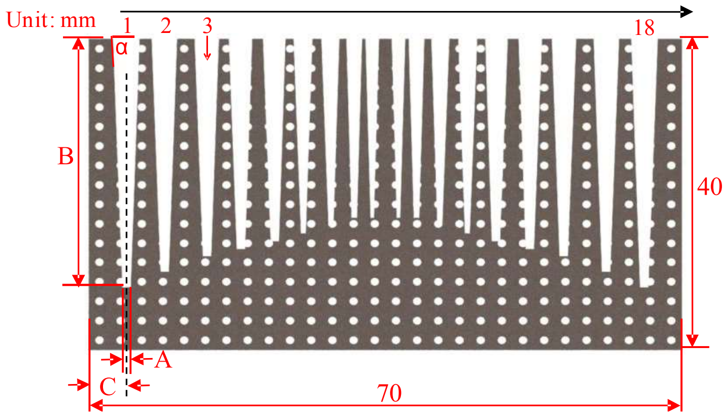

Fig.13. Structural shape of multiple microchannels of nickel foam

Tab.1 Structural parameters of multiple microchannels of nickel foam

Structural parameter \ Microchannel number	1	2	3	4	5	6	7	8	9	10	11	12	13	14	15	16	17	18
A	1	1	1	1	1	0.6	0.6	0.6	0.4	0.4	0.6	0.6	0.6	1	1	1	1	1
B	32	30	28	27	26	25	24	23	23	23	23	24	25	26	27	28	30	32
C	4.5	9	13.75	17.75	21.75	25.175	28.375	31.175	33.5	36.5	38.875	41.625	44.875	48.25	52.25	56.25	61	65.5
α	88°	88°	88°	88°	88°	88°	88°	88°	88°	88°	88°	88°	88°	88°	88°	88°	88°	88°

3.7. Numerical simulation of combustion reaction of nickel foam with multiple microchannels

Fig.14 shows the numerical simulation results of combustion reaction of nickel foam with multiple microchannels. From Figs.12 and 14, it can be seen that compared with the nickel foam without microchannel, the methanol concentration distribution in the nickel foam with multiple microchannels has been changed, and the lower difference in the temperature distribution of the nickel foam under 0.8 mL/min flow rate of methanol is obtained. It reveals the fact that the design of multiple microchannels of nickel foam could decrease the difference in the temperature distribution of nickel foam. Subsequently, a pulsed fiber laser was adopted to secondary process the nickel foam to obtain the nickel foam with the multiple microchannels.

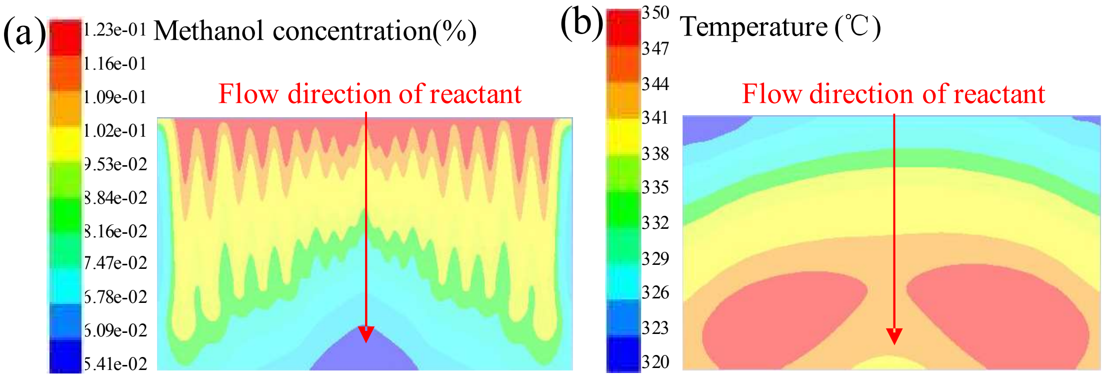

Fig.14. Numerical simulation results of combustion reaction of nickel foam with multiple microchannels: (a) methanol concentration, (b) temperature

3.8. Reaction performance of nickel foam with multiple microchannels

3.8.1 Combustion performance

Fig.15 shows the ΔT_{max} in the temperature distribution of different combustion reaction supports. Compared with the nickel foam without microchannel, the ΔT_{max} in the temperature distribution of the nine points on combustion chamber plate using the nickel foam with multiple microchannels decreases by 57.8% when 1.1 mL/min methanol flow rate is used, which can be seen in Fig.15. The maximum temperature decreases by 33.8 ℃. It is indicated that the design of multiple microchannels of nickel foam is of great significance for decreasing the difference and the maximum in the temperature distribution of the nickel foam.

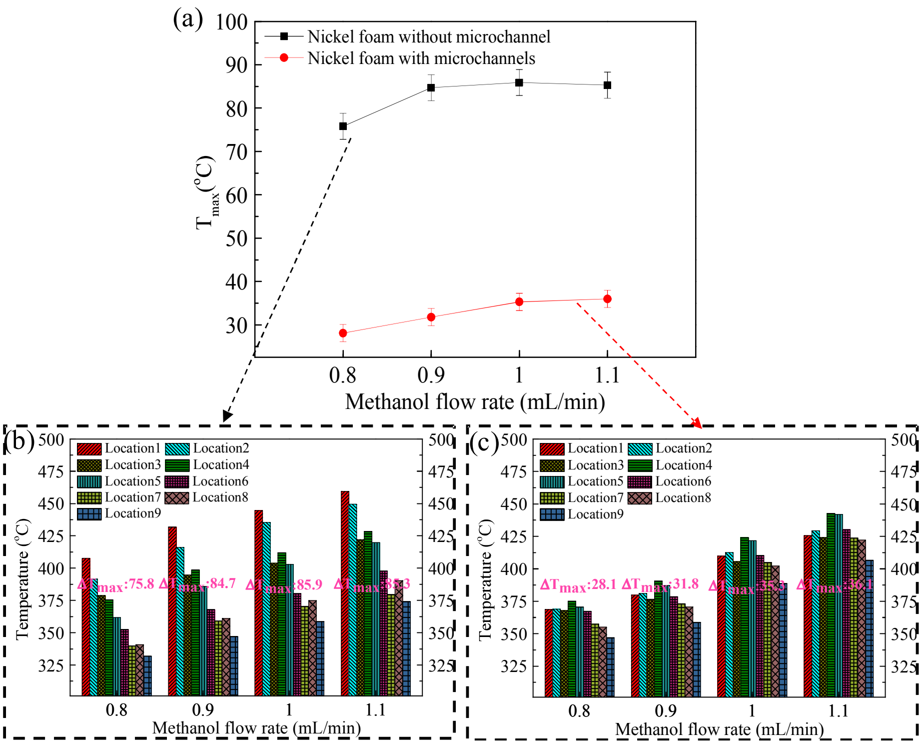

Fig.15. ΔT_{max} in the temperature distribution of different combustion reaction supports: (a) nickel foams without microchannel and with multiple microchannels, (b) nickel foam without microchannel, (c) nickel foam with multiple microchannels

3.8.2 Hydrogen production performance

Fig.16 shows the hydrogen production performances of self-heating methanol steam reforming microreactors using different combustion reaction supports at different reaction conditions. From Fig.16, it can be seen that compared with the nickel foam without microchannel, the self-heating MSR microreactor using the nickel foam with multiple microchannels exhibits better hydrogen production performance. The reforming methanol conversion increases by 21.3% and the H_2 flow rate increases by 21.5% when 430℃ reforming temperature and 4 mL/h flow rate of methanol-water mixture are used. This is mainly due to the fact that compared with the nickel foam without microchannel, the lower difference and the lower maximum in the temperature distribution of combustion chamber plate using the nickel foam with multiple microchannels are existed. Accordingly, the lower difference and the lower maximum in the temperature distribution of reforming chamber plate are obtained. In the process of MSR reaction for hydrogen production, high temperature can easily make the carbon deposit on the surface of the catalyst, reducing the activity of the catalyst. The high temperature will agglomerate the catalyst particles, making the size of catalyst particles be larger and the global catalytic activity area of the catalyst be less. The global reaction performance of the catalyst will decrease. Therefore, the lower difference and the lower maximum in the temperature distribution of reforming chamber plate can prevent the occurrence of the catalyst deactivation in reforming chamber plate[21,41]. The better global catalytic reaction performance of the catalyst in reforming chamber plate can be obtained. In this way, the self-heating microreactor using the nickel foam with multiple microchannels exhibited better hydrogen production performance.

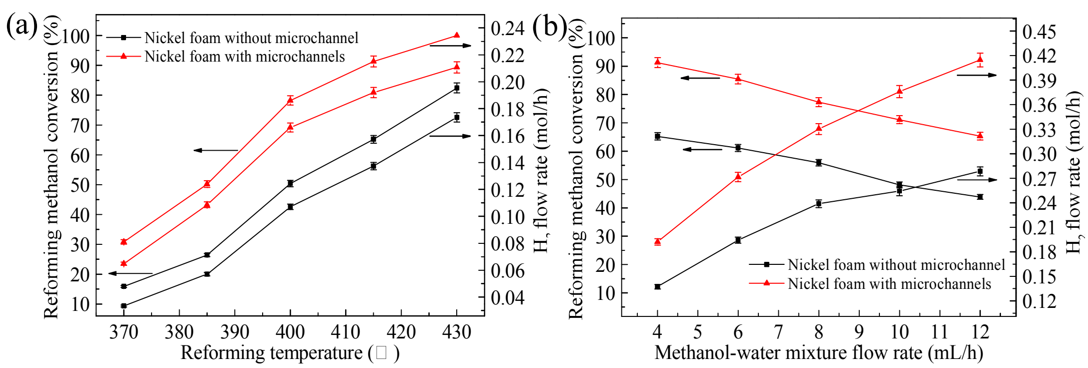

Fig.16. Hydrogen production performances of self-heating methanol steam reforming microreactors using different combustion reaction supports at different reaction conditions (a) different reforming temperatures with 4 mL/h methanol-water mixture flow rate, (b) different methanol-water flow rates with 430℃ reforming temperature

4. Conclusions

To improve the reaction performance of self-heating methanol steam reforming (MSR) microreactor, a nickel foam was used as catalyst support for combustion. A numerical simulation model of combustion reaction of nickel foam was established. The multiple microchannels of the nickel foam were designed based on the numerical simulation results, and some related reaction performances were investigated. It is found that the nickel foam reaction support has a similar temperature distribution with the particles reaction support. In addition, the nickel foam has good long-time combustion stability. Thus, the nickel foam can be used as a combustion reaction support for self-heating MSR microreactor. Compared with the nickel foam without microchannel, the ΔT_{max} and the maximum in the temperature distribution of the nine points of the combustion chamber plate using the nickel foam with multiple microchannels decreased by 57.8% and 33.8 ℃ respectively, when 1.1 mL/min methanol flow rate was used. Compared with the nickel foam without microchannel, the self-heating MSR microreactor using the nickel foam with multiple microchannels exhibited better hydrogen production performance. The reforming methanol conversion increased by 21.3% and the H_2 flow rate increased by 21.5% when 430℃ reforming temperature and 4 mL/h flow rate of methanol-water mixture were used.

Acknowledgments

Thanks to China's National Natural Science Foundation (No.51922092), Natural Science Foundation from Fujian Province of China (No.2017J06015), and Pre-research Project of Equipment in 13th Five-Year of China (No. 41421020103) for supporting this research work .

References

[1] Pan MQ, Feng ZZ, Jiang LB. Reaction characteristics of methanol steam reforming inside mesh microchannel reactor. Int J Hydrogen Energy. 2016;41:1441-52.

[2] Chen F, Chang MH, Kuo CY, Hsueh CY, Yan WM. Analysis of a Plate-Type Microreformer for Methanol Steam Reforming Reaction. Energ Fuel. 2009; 23:5092-98.

[3] Wang XD, Xu X, Wang QL, Huang ZX, He JY, Qiu T. Fatty acid methyl ester synthesis through transesterification of palm oil with methanol in microchannels: flow pattern and reaction kinetics. Energ Fuel. 2020; 34:3628-39.

[4] Mei DQ, Liang LW, Qian M, Feng YB. A performance study of methanol steam reforming in an A-type microchannel reactor. Int J Hydrogen Energy. 2014;31:17690-701.

[5] Yuan W, Su XQ, Zhuang ZU, Huang SM, Wang A, Tang Y. Forced under-rib water removal by using expanded metal mesh as flow fields for air-breathing direct methanol fuel cells. Int J Hydrogen Energy. 2018;43:19711-20.

[6] Ajamein H, Haghighi M, Shokrani R, Abdollahifar M. On the solution combustion synthesis of copper based nanocatalysts for steam methanol reforming: Effect of precursor, ultrasound irradiation and urea/nitrate ratio. J Mol Catal A-Chem. 2016; 421:222-34.

[7] Zhou W, Yu W, Ke YZ, Liu YX, Wan SL, Lin JD. Size effect and series-parallel integration design of laminated methanol steam reforming microreactor for hydrogen production. Int J Hydrogen Energy. 2018;43:19396-404.

[8] Chen JJ, Han JC, Xu DG. Efficient operation of autothermal microchannel reactors for the production of hydrogen by steam methane reforming. Int J Hydrogen Energy. 2019;44:11546-63.

[9] Zhou W, Ke YZ, Wang QH, Wan SL, Lin JD, Zhang JP, et al. Development of cylindrical laminated methanol steam reforming microreactor with cascading metal foams as catalyst support. Fuel. 2017;191:46-53.

[10] Baneshi J, Haghighi M, Ajamein H, Abdollahifar M. Homogeneous precipitation and urea-nitrate combustion preparation of nanostructured $CuO/CeO_2/ZrO_2/Al_2O_3$ oxides used in hydrogen production from methanol for fuel cells. Particul Sci Technol. 2020; 8(4):464-74.

[11] Lotric A, Sekavcnik M, Hocevar S. Effectiveness of heat-integrated methanol steam reformer and polymer electrolyte membrane fuel cell stack systems for portable applications. J Power Sources. 2014;270:166-82.

[12] Tanaka S, Chang KS, Min KB, Satoh D, Yoshida K, Esashi M. MEMS-based components of a miniature fuel cell/fuel reformer system. Chem Eng J. 2004;101:143-49.

[13] Chein RY, Chen YC, Chen JY, Chung JN. Design and test of a miniature hydrogen production reactor integrated with heat supply, fuel vaporization, methanol steam reforming and carbon monoxide removal unit. Int J Hydrogen Energy. 2012;37:6562-71.

[14] Chein RY, Chen YC, Chen JY, Chung JN. Mathematical modeling of hydrogen production via methanol-steam reforming with heat-coupled and membrane-assisted reactors. Chem Eng Technol. 2014;11:1907-18.

[15] Moreno AM, Wilhite BA. Autothermal hydrogen generation from methanol in a ceramic microchannel network. J Power Sources. 2010;195:1964-70.

[16] Yoshida H, Nakajima T, Yazawa Y, Hattori T. Support effect on methane combustion over palladium catalysts. Appl Catal B. 2007;71:70-79.

[17] Chen LX, Mccann JP, Tait SL. A re-examination of the catalyst activation and temperature

hysteresis in methane combustion on Pt/Al_2O_3. Appl Catal A. 2018;549:19-30.

[18] Yu Q, Wang C, Li XY, Li Z, Wang L, Zhang Q, et al. Engineering an effective MnO_2 catalyst from $LaMnO_3$ for catalytic methane combustion. Fuel. 2019;239:1240-45.

[19] Reuse P, Renken A, Haas-Santo K, Gorke O, Schubert K. Hydrogen production for fuel cell application in an autothermal micro-channel reactor. Chem Eng J. 2004;101:133-41.

[20] Hsueh CY, Chu HS, Yan WM, Chen CH. Numerical study of heat and mass transfer in a plate methanol steam micro reformer with methanol catalytic combustor. Int J Hydrogen Energy. 2010;35:6227-38.

[21] Herdem MS, Mundhwa M, Farhad S, Hamdullahpur F. Multiphysics modeling and heat distribution study in a catalytic microchannel methanol steam reformer. Energy Fuel. 2018;32: 7220-34.

[22] Shen CC, Jian TY, Wang YT. Steam reforming of methanol in a compact copper microchannel foam reactor. Fuel Cells; 2013;6:965-70.

[23] Cimino S, Gambirasi A, Lisi L, Mancino G, Musiani M, Vazquez-Gomez L, et al. Catalytic combustion of methanol on Pt-Fecralloy foams prepared by electrodeposition. Chem Eng J. 2016; 285:276-85.

[24] Jin JK, Kwon S. Microcatalytic combustion of H2 on Pt/Al2O3 coated nickel foam. Combust Sci Technol. 2009; 181: 211-25.

[25] Yang HB, Li JC, Yu H, Peng F, Wang HJ. Metal-foam-supported Pd/Al2O3 catalysts for catalytic combustion of methane: effect of interaction between support and catalyst. Int J Chem React Eng. 2015; 13:83-93.

[26] Sesu DC, Patil I, Lokanathan M, Parse H, Marbaniang P, Kakade B. Low density

three-dimensional metal foams as significant electrocatalysts toward methanol oxidation reaction. Acs Sustain Chem Eng. 2018; 6:2062-68.

[27] Ambrosetti M, Balzarotti R, Cristiani C, Groppi G, Tronconi E. The influence of the washcoat deposition process on high pore density open cell foams activation for CO catalytic combustion. Catalysts. 2018; 8,510.

[28] Wang QH, Yang S, Zhou W, Li JR, Xu ZJ, Ke YZ, et al. Optimizing the porosity configuration of porous copper fiber sintered felt for methanol steam reforming micro-reactor based on flow distribution. Appl Energ. 2018;216:243-61.

[29] Zheng TQ, Zhou W, Li XY, You HH, Yang YF, Yu W, et al. Structural design of self-heating methanol steam reforming microreactor with porous combustion reaction support for hydrogen production. Int J Hydrogen Energy. Doi: org/10.1016/j.ijhydene.2020.06.107.

[30] Chen WH, Shen CT, Lin BJ, Liu SC. Hydrogen production from methanol partial oxidation over Pt/Al_2O_3 catalyst with low Pt content. Energy. 2015;88:399-407.

[31] Alvarez-Galvan MC, Navarro RM, Rosa F, Briceño Y, Ridao MA, Fierro JLG. Hydrogen production for fuel cell by oxidative reforming of diesel surrogate: Influence of ceria and/or lanthana over the activity of Pt/Al_2O_3 catalysts. Fuel. 2008;87:2502-11.

[32] Parmar RD, Kundu A, Thurgood C, Peppley BA, Karan K. Kinetic studies of the autothermal reforming of tetradecane over Pt/Al_2O_3 catalyst in a fixed-bed reactor. Fuel. 2010;89:1212-20.

[33] Karim AM, Federici JA, Vlachos DG. Portable power production from methanol in an integrated thermoeletric/microreactor system. J Power Sources. 2008;119:113-20.

[34] Tian JS, Ke YZ, Kong GG, Tan MW, Wang Y, Lin JD, et al. A novel structured PdZnAl/Cu fiber catalyst for methanol steam reforming in microreactor. Renew Energ. 2017;113:30-42.

546 [35] Park GG, Seo DJ, Park SH, Yoon YG, Kim CS, Yoon WL. Development of microchannel methanol steam reformer. Chem Eng J. 2004;101:87-92.

548 [36] Yu H, Chen H, Pan M, Tang Y, Zeng K, Peng F, et al. Effect of the metal foam materials on the performance of methanol steam micro-reformer for fuel cells. Appl Catal A-Gen. 2007;327:106-13.

551 [37] Mei DQ, Feng YB, Qian M, Chen ZC. An innovative micro-channel catalyst support with a micro-porous surface for hydrogen production via methanol steam reforming. Int J Hydrogen Energy. 2016;41:2268-77.

554 [38] Zheng TQ, Zhou W, Yu W, Ke YZ, Liu YX, Liu RL, Kwan SH. Methanol steam reforming performance optimisation of cylindrical microreactor for hydrogen production utilising error backpropagation and genetic algorithm. Chem Eng J. 2019; 357:641-54.

557 [39] Djilali N. Computational modelling of polymer electrolyte membrane (PEM) fuel cells: challenges and opportunities. Energy. 2007;32:269-80.

559 [40] Didari S, Harris TAL, Wei H, Tessier SM, Yan W. Feasibility of periodic surface models to develop gas diffusion layers: a gas permeability study. Int J Hydrogen Energy. 2012;37:14427-38.

561 [41] Twigg MV, Spencer MS. Deactivation of supported copper metal catalysts for hydrogenation reactions. Appl Catal A-Gen. 2001;212:161-74.